Complex formation followed by internal electron transfer: the reaction between L-dopa and iron(III)*

W. Linert**, R. F. Jameson† and E. Herlinger
Institute of Inorganic Chemistry, Technical University of Vienna, Getreidemarkt 9, A-1060 Vienna (Austria)

(Received March 1, 1991; revised May 15, 1991)

Abstract

In anaerobic acid solutions dopa (L-3-(3,4-dihydroxyphenyl)-alanine, H_2LH) reacts with iron(III) to form two complexes, $FeLH^+$ and its protonated form $FeHLH^{2+}$. These both decompose via an intramolecular electron transfer in $FeHLH^{2+}$ to yield iron(II) and dopasemiquinone which in turn is oxidised by iron(III) to dopaquinone. The quinone then cyclises by an intramolecular Michael addition giving the (UV-transparent) leucodopachrome. These reactions have been studied by stopped-flow spectrophotometric, spectroscopic, and chronoamperometric methods, and a mechanism is proposed. Rate constants for the various steps have been evaluated. Spectral data for the complexes and the quinone have also been obtained: $FeLH^+$: maxima at 442 and 700 nm, $\epsilon_{700} = 1380\ M^{-1}\ cm^{-1}$; $FeHLH^{2+}$: maxima at 435 and 660 nm, $\epsilon_{660} = 520\ M^{-1}\ cm^{-1}$; dopaquinone: maximum at 385 nm, $\epsilon_{385} = 1650\ M^{-1}\ cm^{-1}$, shoulder at 458 nm).

1. Introduction

When iron(III) is added to an acidic solution of dopa (L-3-(3,4-dihydroxyphenyl)-alanine) a deep blue and, below a pH of 1.2, a pale green colour appears. Both colours then rapidly fade, but they are restored by the addition of excess iron(II) and, in the case of the blue complex, of base. This behaviour can be observed in many such systems, and it is ascribed to complex formation of the reducible metal ion with the oxidisable ligand, followed by internal electron transfer [1, 2]. In the present case the colours are due to the formation of an 1:1 complex between iron(III) and the dihydroxy function of dopa, the green complex being protonated at one of the co-ordinated oxygen atoms [3]. Up to a pH value of about 2.5 the redox reaction goes to completion, whereas above a pH of about 3 the redox equilibrium is very much in favour of iron(III) complexes (in fact, accurate equilibrium data can be obtained by pH-metric titration methods).

However, under the present conditions, the product of the intramolecular redox process within the iron(III) complexes is the dopaquinone, which in a further reaction step cyclises by an intramolecular Michael condensation to form the UV-transparent leucodopachrome.

The formation of the complex (monitored at 700 nm) is faster than its decomposition by a factor of about 100. Furthermore, the formation and disappearance of the dopaquinone can be followed at 385 nm and is separately accessible by electrochemical methods. This fortunate situation allowed us, by use of high-speed stopped-flow spectrophotometry, to shed light on the rather complicated mechanism of the system and to evaluate rate as well as equilibrium constants.

2. Experimental

Solutions of the required final pH were made up from deoxygenated stock solutions of dopa and of iron(III) that contained calculated amounts of HCl and sufficient KCl to maintain the final ionic strength at 0.10 M; similar solutions containing NO_3^- or ClO_4^- were also used. The pH was measured directly after each kinetic run, and $[H^+]$ was obtained from the experimental pH values in chloride solutions by use of an empirical relationship ($[H^+] = 10^{-\{pH-0.06\}}$) obtained by titrating HCl with KOH. (Note that the concentrations of iron(III) used were so low that changes in pH during reaction were negligible.). All

*Dedicated to Professor V. Gutmann on the occasion of his 70th birthday.

**Author to whom correspondence should be addressed.
†In course of absence from the Department of Chemistry, The University, Dundee DD1 4HN, Scotland, U.K.

0020-1693/91/$3.50

solutions were carefully deoxygenated before use and then transferred from the oxygen-free glove box, where they had been prepared, to the stopped-flow apparatus in sealed syringes.

Spectra of the complex were obtained from a Hitachi U2000-spectrophotometer. Accurate spectral data for the complexes were obtained as follows. Solutions containing 0.01 M dopa, perchloric acid to cover the appropriate pH range, and 0.1 M iron(II) sulphate were made up containing either no added iron(III) to act as reference or known amounts of iron(III) in the range $(1.5\text{–}50)\times10^{-5}$ M. The large excess of iron(II) maintained the equilibrium concentration of the complex by reversing the redox reactions, enabling molar absorbances to be calculated from the spectra.

Kinetic stopped-flow techniques using absorption within the visible and near UV region were carried out with a high speed stopped-flow spectrometer storing some 1016 spectral data points for each spectrum in a multichannel analyser. The multichannel instrument was supplied by Applied Photophysics Ltd. (London). These data were supplemented by more precise kinetic measurements in the near UV region at 385 nm using a conventional monochromatic detector of a Durrum D110 stopped-flow apparatus. The path length of the reaction cell was 2.0 cm in both instruments. All stopped-flow data were obtained with dopa in a large excess enabling them to be treated as pseudo first order reactions. The pH was measured immediately after each run — the very low concentrations of iron(III) employed mean virtually no increase in $[H^+]$ as the reaction proceeds. The background electrolyte was KCl at a total ionic strength of 0.10 M, after preliminary results using KNO_3 and $NaClO_4$ confirmed that the choice of solute did not affect the rate.

Electrochemical investigations were carried out with a conventional galvanostat–potentiostat system supplied by Princeton Applied Research Corporation. The chronoamperometric data [4] were obtained by applying a potential of about 100 mV anodic to peak potential (first obtained by cyclic voltametry) and then following the current–time curves at various pH values.

3. Results and discussion

In the solid, and over a wide pH range in aqueous solution, dopa exists as the zwitterion **I**. In this paper we use the abbreviation H_2LH for this species, i.e. with the phenolic protons written to the left of L and the amino (and carboxyl) protons to the right.

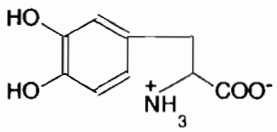

[H_2LH]

I

3.1. Spectra

The spectra of the complex $FeLH^+$, its protonated form $FeHLH^{2+}$, and the quinone are shown in Fig. 1 and gave following characteristics: $FeLH^+$: maxima at 442 and 700 nm, $\epsilon_{700}=1380\ M^{-1}\ cm^{-1}$; $FeHLH^{2+}$: maxima at 435 and 660 nm, $\epsilon_{660}=520\ M^{-1}\ cm^{-1}$. The spectrum of the dopa quinone was obtained directly from the kinetically obtained spectra (λ_{max} 385 nm, $\epsilon_{385}=1650\ M^{-1}\ cm^{-1}$, shoulder at 458 nm). A value of log $K_M^H=1.4$ for the protonation of $FeLH^+$ was obtained from the variation of λ_{max} with $[H^+]$ (A value of 2.9 was previously [5] obtained from potentiometric (pH-metric) measurements but appears to be less reliable because of the redox reaction.)

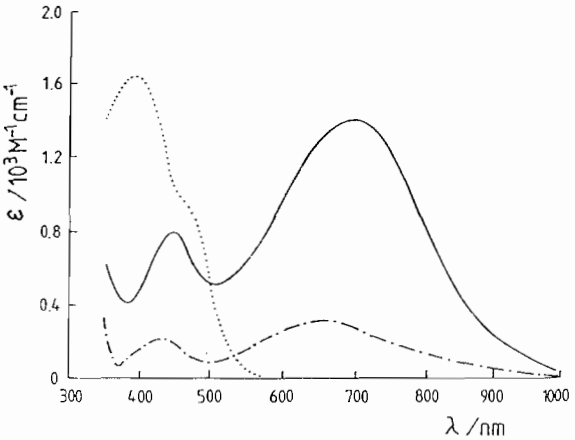

Fig. 1. Electronic spectra of iron(III) complexes of dopa and of dopaquinone: $FeLH^+$ —; $FeHLH^{2+}$ –·–; dopaquinone ·····.

3.2. Protonation constants of dopa

The complete protonation scheme for the dopa anion is given below together with the relevant microconstants [6] ($\mu=0.1$ M KNO_3, 25 °C).

Protonation of phenolic oxygens

$L^{3-}+H^+ \rightleftharpoons HL^{2-}$ log $K_1^H=13.88$

$HL^{2-}+H^+ \rightleftharpoons H_2L^-$ log $K_2^H=8.97$

log $\beta_2^H=\log(K_1^H K_2^H)=22.85$

Protonation of the amino group

$$H_2L^- + H^+ \rightleftharpoons H_2LH \quad \log K_3^H = 9.20$$

Protonation of the carboxyl group

$$H_2LH + H^+ \rightleftharpoons H_2LH_2^+ \quad \log K_4^H = 2.22$$

As these are microconstants their values are not altered by the protonations on other sites. We assume furthermore, that the values for the protonation of the amino and the carboxyl group are insensitive to the reactions of the dihydroxy function, i.e. they are the same for the complex, the quinone and the leucodopachrome.

3.2. *Kinetics*

3.2.1. *Formation of the complexes*

At constant $[H^+]$ the rate of formation of the complexes $FeLH^+$ and $FeHLH_2^+$ was first order in iron(III) concentration (eqn. (1)) over the range pH 1.4–2.6 (i.e. $[H^+] = 0.04$–0.003 M) and was also accurately first order in $[L]_T$. Although the spectra of the differently protonated complex species differ in their molar extinctions the first order character allows us to write eqn. (1) (including both species).

$$d[\text{coloured complex}]/dt = k_1^{obs}[Fe]_T \quad (1)$$

Over this range $k_1^{obs}/[L]_T$ decreased with $[H^+]$ (i.e. increased with pH). Above $[H^+] = 0.04$ M (pH < 1.4) there was a distinct change of the dependence of $k_1^{obs}/[L]_T$ on $[H^+]$, the observed rate increasing as the pH fell. These results are summarised in Fig. 2 where $k_1^{obs}/[L]_T$ is plotted against pH and some typical results are quoted in Table 1.

In a first approximation it is assumed that $Fe(OH)^{2+}$ reacts with dopa regardless of the speciation of the latter. In simplified form this may be written as

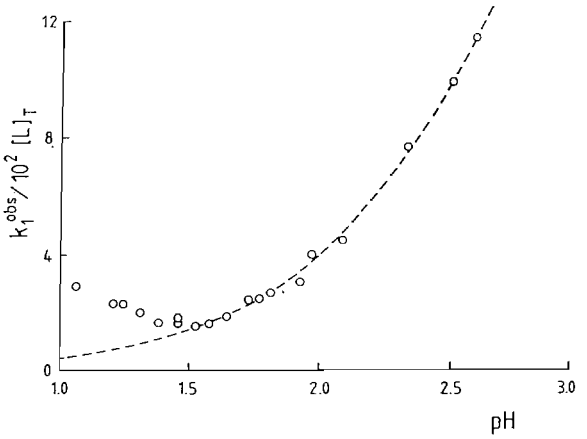

Fig. 2. Formation of the complexes: $k_1^{obs}/[L]_T$ vs. pH. The broken line is computed with $k_1 = 3.13 \times 10^3$ M^{-1} s^{-1}.

$$Fe(OH)^{2+} + \left\{\begin{array}{c} H_2LH \\ \uparrow\downarrow \\ H_2LH_2^+ \end{array}\right\} \xrightarrow{k_1} \left\{\begin{array}{c} FeLH^+ \\ \uparrow\downarrow \\ FeLH_2^{2+} \end{array}\right\} + H^+ + 2H_2O \quad (2)$$

In agreement with the protonation equilibria (see below eqns. (15) and (16)) the shape of the curve in Fig. 2 indicates that above a pH of 1.5 the mainly present coloured complex is $FeLH^+$. The respective rate law thus has the form

$$d([FeLH^+])/dt = k_1[Fe(OH)^{2+}][L]_T \quad (3)$$

Using the equilibrium

$$Fe(OH)^{2+}_{aq} + H^+ \overset{K^{MOH}}{\rightleftharpoons} Fe^{3+}_{aq} \quad (4)$$

and the relationship (5)

$$[Fe]_T = [Fe^{3+}] + [Fe(OH)^{2+}]$$
$$= [Fe(OH)^{2+}](1 + K^{MOH}[H^+]) \quad (5)$$

(3) becomes (6)

$$d(FeHL^+)/dt = k_1[Fe]_T[L]_T/(1 + K^{MOH}[H^+]) \quad (6)$$

Comparison of (6) with (1) and taking reciprocals leads to

$$[L]_T/k_1^{obs} = 1/k_1 + (K^{MOH}/k_1)[H^+] \quad (7)$$

From a plot of $[L]_T/k_1^{obs}$ versus $[H^+]$ both k_1 and K^{MOH} could be determined ($k_1 = (3.13 \pm 0.06) \times 10^3$ M^{-1} s^{-1} and $K^{MOH} = 630$ M^{-1}). Mentasti *et al.* [7, 8] obtained a value of 2.5×10^3 M^{-1} s^{-1} for k_1 and a value of $K^{MOH} = 660$ M^{-1} was previously obtained by us [1, 2] when investigating the analogous reactions with cysteine. That there is no observable curvature in the plot of $[L]_T/k_1^{obs}$ versus $[H^+]$ strongly confirms that the interaction of Fe^{3+} (in contrary to $Fe(OH)^{2+}$) with dopa must be of little importance (as has been implied by (2)) — the rate constant for this reaction cannot in fact be much greater than $10^{-3} \times k_1$ before (7) fails.

Leaving the above simplification, i.e. taking the speciation of dopa into account, the reactions (8) and (9) have to be treated separately

$$Fe(OH)^{2+} + H_2LH \xrightarrow{k_1} FeLH^+ + 2H_2O + H^+ \quad (8)$$

$$Fe(OH)^{2+} + H_2LH_2^+ \xrightarrow{k_2} FeLH^+ + 2H_2O + 2H^+ \quad (9)$$

This implies the rate law

$$d[FeLH^+]/dt = k_1[Fe(OH)^{2+}][H_2LH] + k_2[Fe(OH)^{2+}][H_2LH_2^+] \quad (10)$$

TABLE 1. Typical rate constants for the formation (k_1^{obs}) and decay (k_2^{obs}) of the iron(III) complexes ($[Fe]_T = 1.0–10.0 \times 10^{-5}$ M)

pH	$10^3 \times [H]^+$ (M)	$10^2 \times [L]_T$ (M)	k_1^{obs} (s^{-1})	$k_1^{obs}/10^2 \times [L]_T$ ($M^{-1}\ s^{-1}$)	$10^2 \times k_2^{obs}$ (s^{-1})	$k_2^{obs}/[L]_T$ ($M^{-1}\ s^{-1}$)
1.04	104	1.00	3.06	3.06	2.82	2.82
1.20	72.4	1.25	2.78	2.22	2.79	2.23
1.24	66.1	1.00	2.22	2.22	2.18	2.18
1.31	56.2	0.50	0.97	1.93	0.94	1.88
1.38	47.9	1.00	1.59	1.59	1.55	1.55
1.46	39.8	1.00	1.74	1.74	1.60	1.60
1.53	33.9	1.25	1.76	1.41	1.84	1.47
1.58	30.2	1.00	1.52	1.52	1.48	1.48
1.65	25.7	1.25	2.21	1.77	1.80	1.80
1.77	19.5	0.75	1.76	2.34	2.38	3.17
1.82	17.4	1.00	2.56	2.56	2.91	2.91
1.89	14.8	1.00	2.40	2.40	2.60	2.60
1.93	13.5	1.00	2.84	2.84	3.09	3.09
2.09	9.33	0.50	2.14	4.28	3.58	7.15
2.34	5.25	0.50	3.77	7.54	4.90	9.80
2.52	3.47	1.00	9.70	9.70	10.3	10.3
2.61	2.82	1.00	11.2	11.2	11.9	11.9

In the investigated pH range dopa is almost exclusively present in the forms H_2LH and $H_2LH_2^+$ so that $[L]_T$ is given by eqn. (11)

$$[L]_T = [H_2LH] + [H_2LH_2^+] = [H_2LH](1 + K_4^H[H^+]) \quad (11)$$

Substitution of (5) and (11) into (10) leads to (12)

$$d[FeLH^+]/dt = \frac{(k_1 + k_2K_4^H[H^+])[Fe]_T[L]_T}{\{(1 + K^{MOH}[H^+])(1 + K_4^H[H^+])\}} \quad (12)$$

and comparison of (12) with (1) gives (13).

$$k_1^{obs}/[L]_T = \frac{(k_1 + k_2K_4^H[H^+])}{\{(1 + K^{MOH}[H^+])(1 + K_4^H[H^+])\}} \quad (13)$$

Figure 3 shows a plot of $k_1^{obs}\{(1 + K^{MOH}[H^+])(1 + K_4^H[H^+])\}/[L]_T$ versus $K_4^H[H^+]$ (using the independently obtained values of K^{MOH} [1,2] and K_4^H [6]) which indeed yields a straight line whose slope (3.16×10^3 $M^{-1}\ s^{-1}$) and intercept (3.11×10^3 $M^{-1}\ s^{-1}$) correspond to k_2 and k_1, respectively. It is remarkable [9] that, despite the fact that the two dopa species present are differently charged, the two rate constants are almost identical, in turn giving significance to the former simplified treatment. Using these results the broken line in Fig. 2 has been calculated showing that the identification of $FeLH^+$ as the coloured species above a pH of 1.5 is valuable. The rise in $k_1^{obs}/[L]_T$ below this pH can be attributed to increasing importance of the back reaction. Using the equilibria of complex formation and protonation,

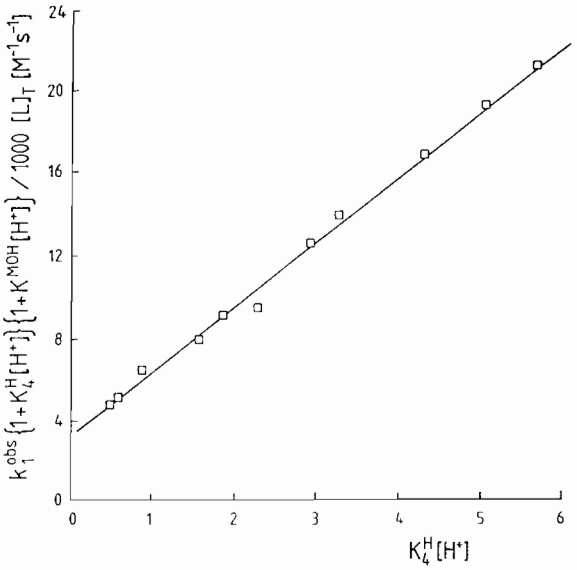

Fig. 3. Plot of $k_1^{obs}\{(1 + K^{MOH}[H^+])(1 + K_4^H[H^+])\}/[L]_T$ vs. $K_4^H[H^+]$, with intercept $= k_1 = 3.11 \times 10^3$ $M^{-1}\ s^{-1}$ and slope $= k_2 = 3.16 \times 10^3\ M^{-1}\ s^{-1}$, indicating the independence of the rate of formation on speciation of dopa. Derivation given in the text.

one can calculate that below this pH the reaction no longer goes to completion. Therefore it is necessary to include the back reactions in the above reaction schemes. Unfortunately our results in this range are not accurate enough to get quantitative results although the rise in rate can be qualitatively reproduced.

3.2.2. Rate of decomposition of the complexes

At constant $[H^+]$ and $[L]_T$ the rate of decomposition is given by (14)

$$-d[\text{coloured complex}]/dt = k_2^{obs}[Fe]_T \quad (14)$$

The rate is first order in $[L]_T$ and results are summarised in Fig. 4 and typical $k_2^{obs}/[L]_T$ are given in Table 1. It might be pointed out that the observed first order dependence is not simply explicable by the excess in dopa used to obtain pseudo first order kinetics for the preceding complex formation. As seen below the decomposition of the complex does not involve dopa as a reactant. However, the concentration of the complex itself depends upon $[L]_T$.

Above pH = 1.30 the results can be explained by eqns. (15)–(18) in which °HLH is the dopasemiquinone.

$$FeLH^+ + H^+ \overset{K_M^H}{\rightleftharpoons} FeHLH^{2+} \quad (15)$$

$$FeHLH^{2+} + H^+ \overset{K}{\rightleftharpoons} FeHLH_2^{3+} \quad (16)$$

$$FeHLH^{2+} \xrightarrow{k_3} Fe^{2+} + {}^\circ HLH \quad (17)$$

$$FeHLH_2^{3+} \xrightarrow{k_4} Fe^{2+} + {}^\circ HLH + H^+ \quad (18)$$

$$-d[FeLH^+]/dt = k_3[FeHLH^{2+}] + k_4[FeHLH_2^{3+}] \quad (19)$$

i.e. we allow for protonation of the carboxyl group. We now assume that the value of K is equal to the respective value for dopa, K_4^H, and that the protonation reactions of $FeLH^+$ (15) and $FeHLH^{2+}$ (16) are fast, compared with the decomposition reactions. (19) then becomes (20)

$$-d[FeLH^+]/dt = (k_3 + k_4K_4^H[H^+])K_M^H[FeLH^+][H^+] \quad (20)$$

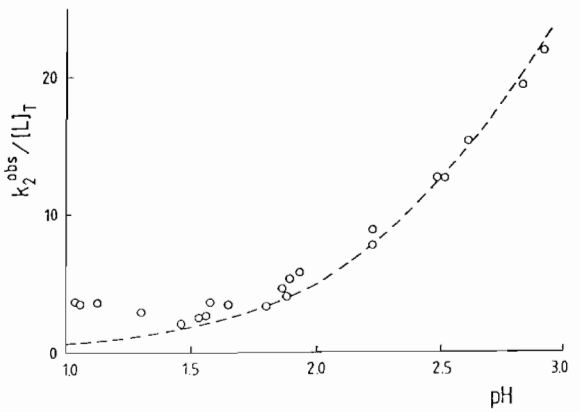

Fig. 4. Decomposition of the complexes: $k_2^{obs}/[L]_T$ vs. pH. The broken line is computed with $k_3K_M^H = 7.52\ M^{-1}\ s^{-1}$.

and, as has been shown above in the case of the formation of the complexes, it is probable that both k_3 and k_4 are equal. Hence (20) reduces to (21).

$$-d[FeLH^+]/dt = k_3K_M^H(1 + K_4^H[H^+])[FeLH^+][H^+] \quad (21)$$

Making use of (5), (11) and the appropriate equilibrium constants, and defining an equilibrium constant K_1^M (22)

$$Fe^{3+} + LH^{2-} \overset{K_1^M}{\rightleftharpoons} FeLH^+ \quad (22)$$

(21) becomes (23)

$$-d[FeLH^+]/dt = \{k_3K_M^HK_1^MK^{MOH}/\beta_2^H \times (1 + K^{MOH}[H^+])\}[Fe]_T[L]_T \quad (23)$$

Comparison of (23) with (14) together with the fact that $2d[FeLH^+]/dt = d[Fe]_T/dt$ (due to the fast reaction of the semiquinone produced with another iron(III) ion (*vide infra*)) and taking the reciprocal leads to (24) and a plot of $[L]_T/k_2^{obs}$ versus $[H^+]$ enables K^{MOH} to be obtained from slope/intercept ($K^{MOH} = 630$, identical to that obtained for the formation of $FeLH^+$, above) and $k_3K_M^H = \beta_2^H/(K_1^M \times$ slope). Use of the accepted values [6] for β_2^H and K_1^M yields $k_3K_M^H = 7.52 \pm 0.15\ M^{-1}\ s^{-1}$ in good agreement with the value of Mentasti *et al.* [8] of 3.89 $M^{-1}\ s^{-1}$ for half the rate constant. k_3 itself can be obtained using the rather insensitive value of $K_M^H = 25 \pm 2.5\ M^{-1}$ to give $0.30 \pm 0.05\ s^{-1}$.

$$[L]_T/2k_2^{obs} = \beta_2^H/k_3K_M^HK_1^MK^{MOH} + (\beta_2^H/k_3K_M^HK_1^M)[H^+] \quad (24)$$

The increase in rate observed below a pH of about 1.30 can be explained as follows. The actual decomposition of $FeLH^+$ proceeds almost certainly via rapid protonation to form $FeHLH^{2+}$ which then slowly decays. Below pH = 1.3 the concentration of $FeHLH^{2+}$ begins to rise at the expense of $FeLH^+$, since the total concentration of the complex decreases with decreasing pH. As now the concentration of the rate determining species increases the speed of the reaction and the *observed* rate constant increase, as can be seen in Fig. 4.

3.2.3. Formation of the dopaquinone

In contrary to earlier reports the appearance of dopaquinone does not simply follow the disappearance of the complex species [8]. The formation of the quinone, QH (**II**), followed at 385 nm, yields what appears to be biphasic kinetics. At low pH

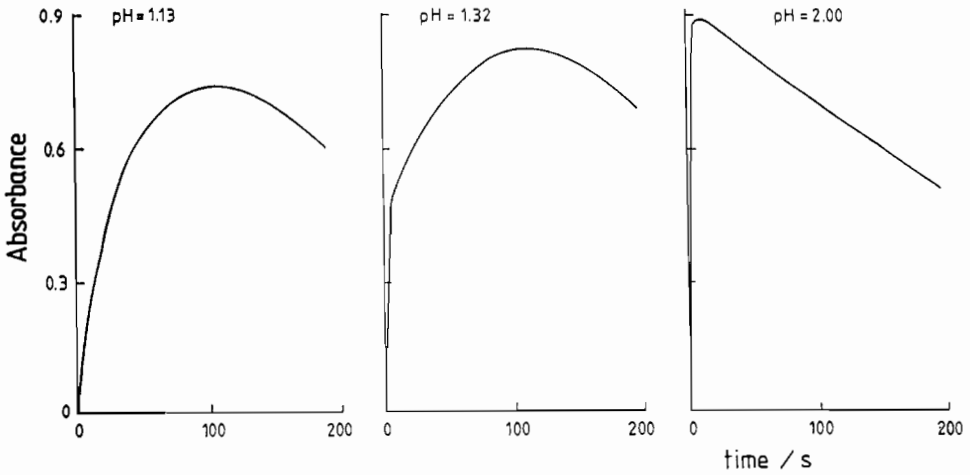

Fig. 5. Formation of dopaquinone: increased appearance of fast formation step as pH increases.

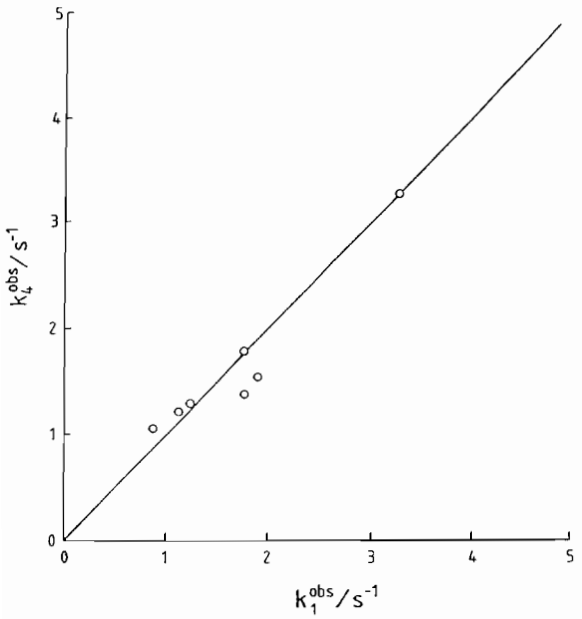

Fig. 6. Relationship between the fast rate of formation of dopaquinone (k_4^{obs}) and the rate of formation of the complexes (k_1^{obs}) (line drawn with unit slope).

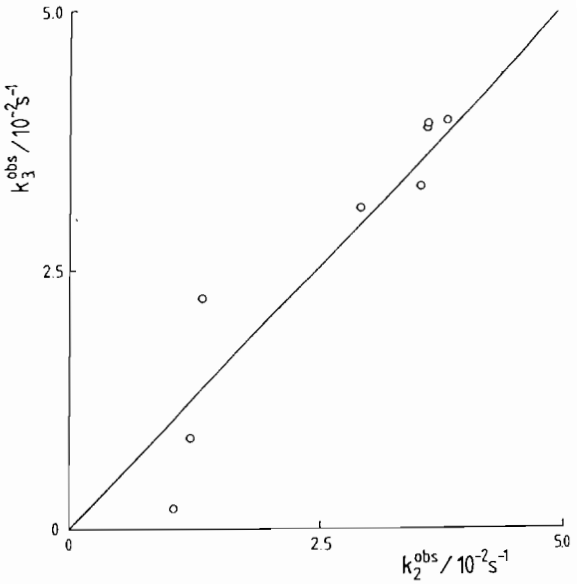

Fig. 7. Relationship between the slow rate of formation of dopaquinone (k_3^{obs}) and the rate of formation of the complexes (k_2^{obs}) (line drawn with unit slope).

values there is a single relatively slow formation step of the quinone, but as the pH is increased this is preceded by a fast formation step until by pH of 1.8 only the fast step is observed (Fig. 5).

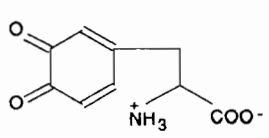

Dopaquinone (QH)

II

The present investigation shows that the occurrence of biphasic kinetics does not necessarily point to a two step mechanism. From the electronic spectra (Fig. 1) it is known that beside the quinone the formed complexes also absorb near 385 nm. Keeping this in mind, the observed behaviour and its dependence on the pH values can be explained as follows.

(i) Fast formation kinetics. In this case the rate of formation of QH is again of the form (25) and is exactly equal to the rate of formation of $FeLH^+$

$$d[QH]/dt = k_4^{obs}[Fe]_T \qquad (25)$$

k_4^{obs} is exactly equal to the rate of formation of $FeLH^+$ as is shown in Fig. 6. Examination of the spectra (Fig. 1) together with the fact that at these pH values $[FeLH^+]$ is formed in increasing amount, leads us to the conclusion that it is this species that we are following, and not [QH].

(ii) Slow formation kinetics. The rate equation at constant $[H^+]$ and $[L]_T$ takes the form (26) and is first order in $[L]_T$

$$d[QH]/dt = k_3^{obs}[Fe]_T \quad (26)$$

The rate constants obtained reflect the *decomposition* of $FeLH^+$ (see Fig. 7) and so the reaction scheme (27) is proposed.

$$FeHLH^{2+} \xrightarrow{k_3} Fe^{2+} + {}^{\circ}HLH$$

$$FeHLH_2^{3+} \xrightarrow{k_4} Fe^{2+} + {}^{\circ}HLH + H^+$$

$$Fe^{3+} + {}^{\circ}HLH \xrightarrow{fast} QH + Fe^{2+} + H^+ \quad (27)$$

This leads to (28) which is the required result

$$d[QH]/dt = k_3[FeHLH^+] + k_4[FeHLH_2^{2+}] = k_2^{obs}[Fe]_T \quad (28)$$

3.2.4. Cyclisation of dopaquinone

It is well established [10, 11] that the quinone of dopa and related substances (e.g. adrenaline) spontaneously cyclise via a Michael addition to form the UV-transparent leucodopachrome (**III**).

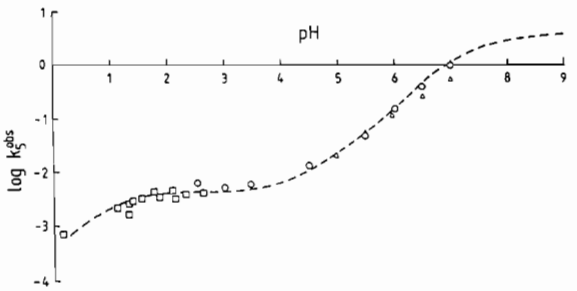

Fig. 8. Observed rates of cyclisation of dopaquinone to form leucodopachrome: □ = kinetic results for dopa; ○ = chronoamperometric results for dopa; △ = chronoamperometric results for α-methylnoradrenaline. The derivation of the curve is given in the text.

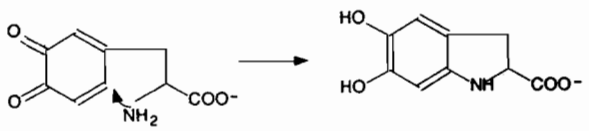

III (29)

The kinetics of this cyclisation were established by monitoring the quinone at 385 nm. This was possible because at very low pH the spectral absorption of the quinone rapidly exceeded that of the complex. At higher pH values this was no longer the case and the formation of the quinone could not be followed. Its disappearance, however, could be followed since iron(II) does not absorb appreciable at this wavelength.

The rate of disappearance of the quinone is given by

$$-d[Q]_T/dt = k_5^{obs}[Q]_T \quad (30)$$

Typical first order rate constants obtained for the decay of the quinone at various pHs are listed in Table 2 and included in Fig. 8. The values appeared to be surprisingly high when compared with those for the rate of cyclisation of α-methylnoradrenaline obtained by chronoamperometry by Hawley *et al.* (Fig. 3 in ref. 12 was redrawn using those values) and which we expected to be similar to those of dopa. We therefore used the same technique as Hawley *et al.* in order to obtain pH dependent data for the cyclisation of dopaquinone and these are presented in Table 3 and Fig. 8 together with those for α-methylnoradrenaline. The figure shows how they confirm that our results do indeed refer to the cyclisation reaction.

To explain these results we postulate the following reaction scheme (31) in which K_0 is the microconstant for the protonation of the carboxyl group in dopaquinone and leucodopachrome (The proton at the carboxyl site is indicated by H_0).

In other words we propose that the lower rates at low pH values are due to the protonation of the carboxyl group and the theoretical curve included in Fig. 8 was derived on this basis as follows.

We assume that the reactive species is deprotonated at the amino site, and because the protonation constant of this group is high, i.e.

TABLE 2. Typical values for the observed rate constants (k_5^{obs}) obtained for the cyclisation of dopaquinone to leucodopachrome (kinetic data)

pH	0.15	1.12	1.32	1.55	1.76	1.85	2.07	2.30
$-\log k_5^{obs}$	3.15	2.62	2.59	2.49	2.35	2.46	2.34	2.41

TABLE 3. Values of the rate constants (k_5^{obs}) for the cyclisation of dopaquinone to leucodopachrome obtained by chronoamperometry

pH	3.50	4.50	5.50	6.00	6.50	7.00
$-\log k_5^{obs}$	2.35	2.11	1.22	0.77	0.30	0.11

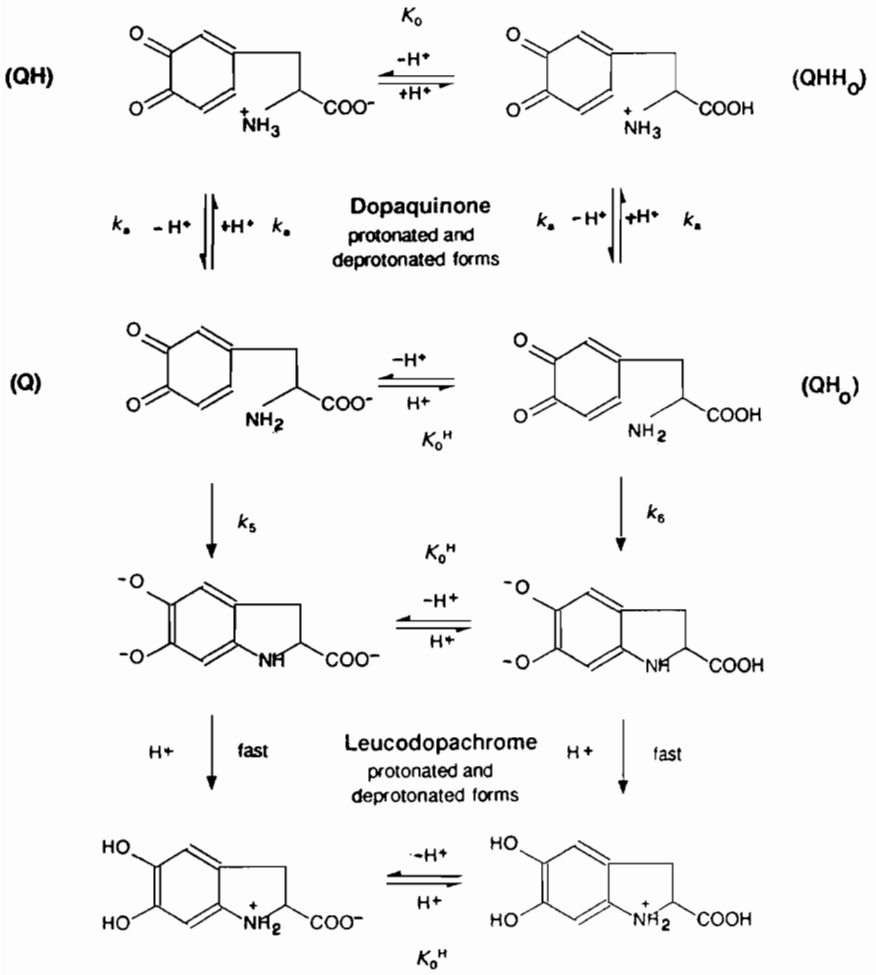

(31)

$$RNH_2 + H^+ \underset{k_{-a}}{\overset{k_a}{\rightleftharpoons}} RNH_3^+ \tag{32}$$

$$K_N^H = k_a/k_{-a} = [QH]/[Q][H^+] \tag{33}$$

the deprotonation step is relatively slow and must be included in the reaction scheme. (We also assume that k_{-a} is independent of protonation at the carboxyl site.)
Thus we have

$$-d[Q]_T/dt = k_5[Q] + k_6[QH_0] \tag{34}$$

$$= (k_5 + k_6 K_0^H [H^+])[Q] \tag{35}$$

but under these conditions [Q] would reach a steady state, i.e.

$$d[Q]/dt = 0 \tag{36}$$

which yields

$$k_{-a}[QH] = k_a[Q][H^+] + k_5[Q] \tag{37}$$

i.e.

$$[Q] = [QH]/\{K_N^H[H^+] + k_5/k_{-a}\} \tag{38}$$

The total quinone concentration is given by (39) and (40) and

$$[Q]_T = [QH] + [QHH_0] \quad (39)$$

$$= [QH]\{1 + K_0^H[H^+]\} \quad (40)$$

hence substitution for [QH] from (40) in (38) and comparing the results with (30) yields (41).

$$k_5^{obs} = (k_5 + k_6 K_0^H[H^+])/\{(K_N^H[H^+] + k_5/k_{-a})(1 + K_0^H[H^+])\} \quad (41)$$

(Based on the experience with microconstants [6] K_N^H and K_0^H were assumed to have the same value as the corresponding protonation constants for dopa, viz. K_0^H = microconstant for the protonation of COO^-, log $K_4^H = 2.22$; K_N^H = microconstant for the protonation of $-NH_2$, log $K_3^H = 9.20$.)

The best fit to the observed data was obtained with $k_{-a} = 3.42 \pm 0.08\ s^{-1}$; $k_5 = (1.41 \pm 0.04) \times 10^2\ s^{-1}$; $k_6 = (4.8 \pm 0.1) \times 10^4\ s^{-1}$.

4. Conclusions and general discussion

Under anaerobic conditions four general steps of the present redox reaction between Fe(III) and dopa could be followed spectrophotometrically, namely (i) the formation of a complex between the metal ion and protonated and unprotonated species, (ii) the decomposition of the complex after electron transfer, yielding Fe(II) and dopasemiquinone, (iii) the formation of dopaquinone (directly observable at low pH), and (iv) its cyclisation via an intramolecular Michael addition yielding leucodopachrome. Chronoamperometric investigations allowed to investigate the cyclisation step independently. In the presence of oxygen further oxidations occur, yielding dopachrome and finally melanine.

The rate constant obtained largely confirm those of Mentasti *et al.* [7], but the interpretation differs in two important ways. Firstly our results clearly show that even at low pH values the reaction proceeds exclusively via complex formation. Secondly our results show that the complex $FeLH^+$ is protonated at one of the coordinated phenolic oxygen atoms (as has been well established in the case of tiron [3]). It is the protonated complex, $FeHLH^{2+}$, that relatively slowly decomposes by intramolecular electron transfer from dopa to coordinated iron(III). It should be pointed out that *all* the kinetics involving the complex are governed by its concentration. The increase in k_2^{obs} above a pH of 1.3 is due to this fact as is the formation of the quinone.

The fact that we were able to follow the cyclisation reaction of the dopaquinone to leucadopachrome at very low pH values is also of some importance since below a pH of about 3 the chronoamperometric method is not successful [12]. Thus a expansion of the range – either pH or k^{obs} – of electrochemical methods by stopped-flow methods is possible.

It is perhaps surprising that protonation of the carboxyl group of the dopaquinone has such a strong effect, but we ascribe this to the breaking of a hydrogen bond between the unprotonated amino group and the anionic form of the carboxyl group on protonation of the latter.

Acknowledgements

Thanks are due to the Fonds zur Förderung der wissenschaftlichen Forschung in Österreich (Project 7605). Professor V. Gutmann is thanked for giving his continual support for these investigations.

References

1 R. F. Jameson, W. Linert, A. Tschinkowitz and V. Gutmann, *J. Chem. Soc., Dalton Trans.*, (1988) 943.
2 R. F. Jameson, W. Linert and A. Tschinkowitz, *J. Chem. Soc., Dalton Trans.*, (1988) 2109.
3 G. Schwarzenbach and A. Willi, *Helv. Chim. Acta, 34* (1951) 528.
4 M. D. Hawley and S. W. Feldberg, *J. Phys. Chem., 70* (1966) 3459.
5 J. E. Gorton and R. F. Jameson, unpublished results.
6 R. F. Jameson, G. Hunter and T. Kiss, *J. Chem. Soc., Perkin Trans. 2,* (1980) 1105.
7 E. Mentasti, E. Pelizzetti and G. Saini, *J. Inorg. Nucl. Chem., 38* (1976) 785.
8 E. Mentasti, E. Pelizzetti and C. Baiocchi, *J. Inorg. Nucl. Chem., 38* (1976) 2017.
9 K. J. Laidler, *Chemical Kinetics,* Mc Graw-Hill, New York, 2nd edn., 1965, p. 220.
10 J. D. O'Bu'Lock and J. Harley-Mason, *J. Chem. Soc.,* (1951) 712.
11 R. A. Heacock, *Chem. Phys., 59* (1959) 181.
12 M. D. Hawley, S. V. Tatawawadi, S. Piekarski and R. N. Adams, *J. Am. Chem. Soc., 89* (1967) 447.